LITE Flood: Simple GIS-Based Mapping Approach for Real-Time Redelineation of Multifrequency Floods

Farid Javadnejad, S.M.ASCE[1]; Brian Waldron, Ph.D., P.E., M.ASCE[2]; and Arleen Hill, Ph.D.[3]

Abstract: Flood zones with 1 and 0.02% of annual flooding chance are projected in FEMA's digital flood insurance rate maps (DFIRMs) and are suited for identifying flood risk at the largest impacts. However, less severe floods, which are not mapped in DFIRMs, still cause significant damage and occur on a more frequent basis. This article uses a simplified rapid geographic information system (GIS)-based solution for on-the-fly inundation mapping of small flood events. The linear interpolation technique (LITE Flood) was developed to approximate the prone flood zones based on river stage without performing additional hydraulic simulations. The approach was evaluated by comparing the results to the corresponding storm scenarios simulated in a standard river hydraulics simulator. The case study is a portion of Wolf River and its two main tributaries in Shelby County, which is located in the southwest corner of Tennessee. The stream channelization of the lower portion of Wolf River has mitigated large flood events, while causing frequent flooding from less severe storms. LITE Flood produced results with good to acceptable accuracy. LITE Flood can be used for rapid, cost-effective, and real-time mapping of multifrequency floods at a large scale, thereby aiding local community emergency response agencies who often do not have the expertise to perform more sophisticated hydraulic modeling but do have a GIS capacity. **DOI: 10.1061/(ASCE)NH.1527-6996.0000238.**

Author keywords: Floods; Flood mapping; Real-time; Redelineation; *Hydrologic engineering center–river analysis system (HEC-RAS)*; Geographic information system (GIS).

Introduction

Floods are the most common and most deleterious natural disaster in the United States in terms of lost lives and damage to properties and infrastructures (FEMA 2016). On average, about two-thirds of federal disaster declarations are related to flooding [Fig. 1(a); USGS 2013]. FEMA is responsible for identifying a number of artificial and natural disasters, in particular, assessing flood hazard (FEMA 2015a). Started in 1968, the National Flood Insurance Program (NFIP) requires FEMA to seek effective ways to reduce flood damages and costs through analyzing the flood hazard and providing individuals, businesses, and communities with flood management practices (FEMA 2015a). For a large number of densely populated counties in the United States, FEMA's digital flood insurance rate maps (DFIRMs) are the most current and reliable flood inundation delineations for specific large flood events [Fig. 1(b); FEMA 2002, 2015a].

DFIRMs are available as digital map images and also exist in geographic information system (GIS) format, providing the users with delineated floodplain boundaries and areal extents of flooding attributable to storm events with a 1 and 0.2% probability of occurring in one year (often referred to as the 100- and 500-year floods, respectively) (FEMA 2002, 2013b). However, small flood events that do not reach the magnitude of a 100-year or higher event flood still cause significant damage and occur on a more frequent basis. Therefore, it is within the purview of local emergency response agencies to plan for the societal impacts of more frequent floods than the 100- or 500-year events (FEMA 2010).

The European Union launched the European Exchange Circle on Flood Mapping Program (EXCIMAP) that identifies multiple flood hazard zones (e.g., high, medium, low, and residual risk) in a number of its member countries (EXCIMAP 2007). In the United States, the advanced hydrologic prediction service (AHPS) offers animated flood maps with high, medium, and low risks at a number of locations (NOAA 2011). With FEMA mapping, the less severe floods (e.g., 10- and 50-year return periods) are simulated in some of the original hydraulic models (FEMA 2005); however, the resulting flood inundation extents are not mapped in the DFIRMs. Accordingly, FEMA is beginning to look into the consequences of smaller flood events through its risk mapping, assessment, and planning (Risk MAP) program (FEMA 2010, 2013b, 2015b).

In the aforementioned mapping efforts, determination of flood inundation extents for the more frequent events requires hydraulic numerical modeling of the river system. Developing flood inundation maps using hydraulic simulators is an expensive procedure in terms of data collection, design, computation, and professional costs. Emergency response agencies, especially in rural areas such as those adjacent to Shelby County, Tennessee, have limited financial and technical sources for flood inundation mapping using a numerical approach. Additionally, the process of reconstructing the numerical models used to create the DFIRMs has its own challenges, because for a single river system, numerous numerical models were developed at different times. This means these models may include multiple river sections and contain varying inputs that make compilation of all hydraulic models into a unified model for the entire river network a challenging task.

Although guidelines and regulations require the use of hydraulic models to map flood extent (FEMA 2002), there are applications of nonhydraulic or quasi-hydraulic models that can address the need

[1]Graduate Research Assistant, School of Civil and Construction Engineering, Oregon State Univ., 101 Kearney Hall, Corvallis, OR 97331 (corresponding author). E-mail: fjnejad@lifetime.oregonstate.edu

[2]Associate Professor, Dept. of Civil Engineering, Univ. of Memphis, 110D Engineering Science Bldg., Memphis, TN 38152. E-mail: bwaldron@memphis.edu

[3]Associate Professor, Dept. of Earth Sciences, Univ. of Memphis, 109 Johnson Hall, Memphis, TN 38152. E-mail: aahill@memphis.edu

Note. This manuscript was submitted on January 15, 2016; approved on September 16, 2016; published online on January 25, 2017. Discussion period open until June 25, 2017; separate discussions must be submitted for individual papers. This paper is part of the ***Natural Hazards Review***, © ASCE, ISSN 1527-6988.

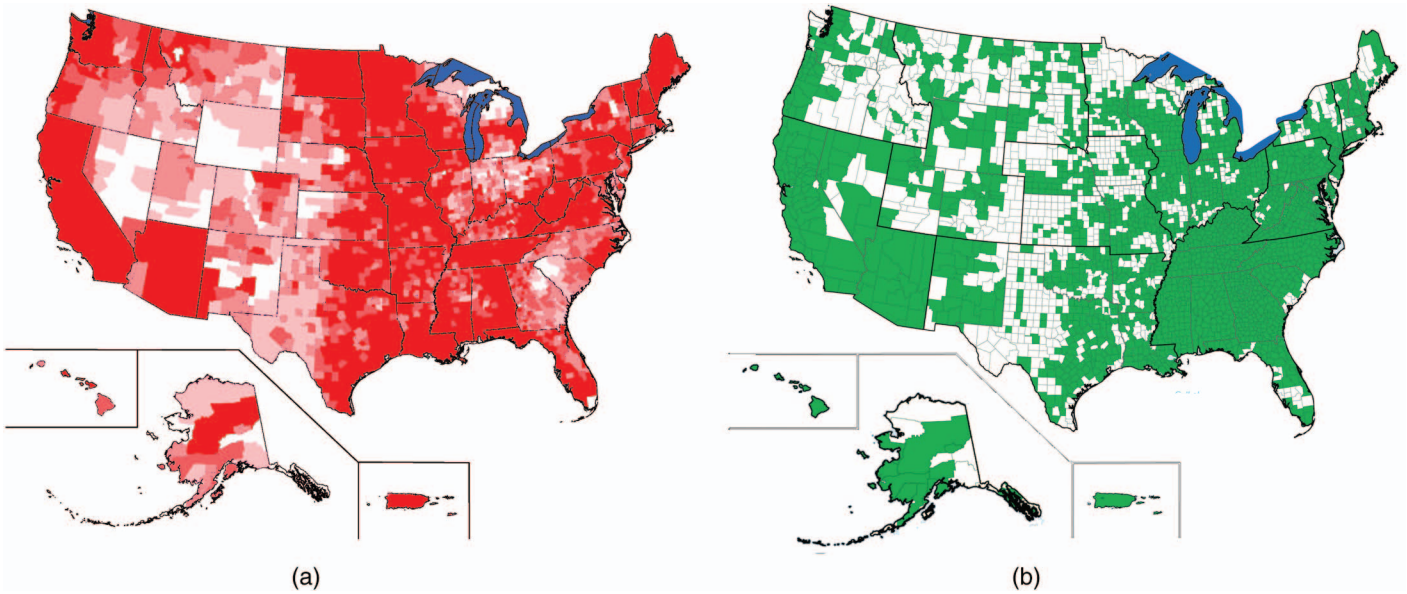

Fig. 1. (Color) (a) Presidential disaster declarations related to flooding: very light, light, dark, very dark shaded areas represent counties with one, two, three, and four or more declarations, respectively, since 1965–2003 (modified from USGS 2006); (b) FEMA's preliminary DFIRMs available nationwide as of September 2011 (shaded areas); note: maps are not to scale

of preparedness planners when detailed models and data are not available (Dickerson 2007; Gall et al. 2007; Verdin et al. 2016). In areas where flood risk is expected to stay unaltered, *redelineation* of effective data without performing new hydraulic modeling can be a time and cost-effective alternative (NRC 2007). Looking for alternative approaches in the absence of detailed hydrologic and hydraulic data, Gall et al. (2007) adopted the USGS's stream flow model (SFM) and FEMA's natural hazard loss estimation software (HAZUS-MH) for flood mapping, although neither of these models are designed and widely used for floodplain mapping.

GIS-based techniques are of great interest owing to the ease of use and availability of software and technical resources, as well as development and computation costs. There are numerous GIS approaches that provide solutions for spatial problems by simplifying the model assumptions, e.g., geological remote sensing (Molan and Behnia 2013), health mapping in developing countries (Fisher and Myers 2011), landslide hazard mapping (M. Sharifi-Mood et al., "Performance-based, seismically-induced landslide hazard mapping of west Oregon," submitted, *Soil Dyn. Earthquake Eng.*, Elsevier, Amsterdam, Netherlands), land-use suitability analysis (Malczewski 2006), mineral potential mapping (Javadnejad et al. 2013), sediment pathway estimation (Kiesel et al. 2009), traffic noise mapping (Ozdenerol et al. 2015), tornado damage assessment (Kashani et al. 2015b), and water balance and hydrological modeling (Van Der Knijff et al. 2010). These approaches try to alleviate the need for sophisticated or costly modeling by minimizing the number parameters in the models, while optimizing the complexity of the model or amount of field measurements.

Obtaining simple and reliable solutions for mapping flood event inundation extents that match the capability and resources of nontechnical emergency response agencies is of great interest. Recently, USGS launched a GIS Flood Tool (GFT), for rapid flood hazard assessment in developing countries (Verdin et al. 2016). GFT operates by defining the depth-discharge relationship using Manning's (1891) equation at user specified cross sections and a digital elevation model (DEM), which is later used to estimate water depth for a given discharge value at a river segment. Using the relative DEM analysis, the tool maps the inundated zones. GFT can be perceived as erroneous because it does not require any prior hydraulic mapping; however, it suits well for approximating reconnaissance-level estimates of inundation zones in areas with limited resources and data (Verdin et al. 2016).

The linear interpolation technique of flood mapping (LITE Flood) was developed, which is a simplified GIS tool for mapping smaller flood events. LITE Flood is applicable to areas where base flood events using preliminary hydrologic and hydraulic modeling [e.g., Fig. 1(b)] have attained prior, yet development and calibration of these models for smaller events proves time consuming and real-time mapping is demanded. LITE Flood is viable through the widely used and easily accessible GIS software packages. LITE Flood is developed based on the interpolation of water surface elevations (WSE) for the stage level of an intermediate flood between upper and lower water surface boundaries. In this technique, the size of a flood was defined using the river stage at the reference stations, which is already impacted by volume and duration. The resulting WSEs were compared with topography to map the effective inundated areas. The LITE Flood was examined in a case study of the Wolf River and its two main tributaries, and the accuracy was assessed by comparing the results to the corresponding flood events modeled by FEMA using the recommended Hydrologic engineering center–river analysis system (*HEC-RAS*) numerical modeling software.

Methodology

The GIS-based LITE Flood technique was used to estimate flood inundation extents for storms of greater recurrence frequency than the 100-year flood. The linear interpolation of WSEs from a base flood event (100-year storm) was used to create flood maps of smaller (10- and 50-year) events with respect to a known stage level at a reference location. To evaluate this approach, the results were compared to those of standard hydraulic-based flood mapping Emeganausing *HEC-RAS* (version 4.1) and incorporating FEMA's original hydraulic models. Initial model calibration is performed by matching simulated WSEs from a 100-year storm event ($WSE_{100-year}$) with that from the FEMA DFIRM. Once the

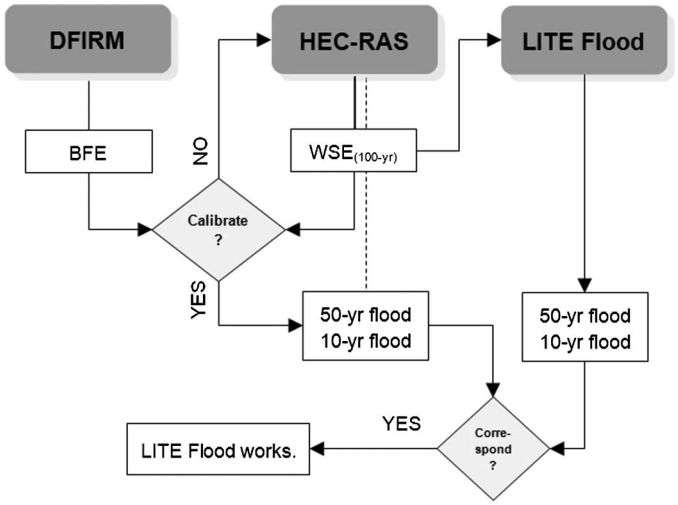

Fig. 2. Study approach for development, calibration of hydraulic models, and assessment of GIS-based LITE Flood approach for multifrequency flood mapping

numerical model was calibrated, varying flood scenarios up to the 100-year flood event were modeled using *HEC-RAS*. The *HEC-RAS* results were then compared to the flood elevations and extent of the same scenario derived from the LITE Flood procedure. Fig. 2 shows the scheme of study approach.

HEC-RAS

The floodplain modeling techniques are categorized into three major groups of one- (1D), two- (2D), and three-dimensional (3D) models. 1D models are more appropriate for planning, management, and flood protection purposes at big catchment and subcatchment scales (Pender and Néelz 2007; Yang et al. 2012; Dimitriadis et al. 2016).

HEC-RAS is a software package developed by the Hydrologic Engineering Center (HEC) of the U.S. Army Corps of Engineers (USACE) (Brunner 2016). It is dominantly used for 1D hydraulic modeling. FEMA lists *HEC-RAS* as one of the accepted hydraulics models for flood mapping (FEMA 2015a). *HEC-RAS* is capable of performing 1D steady and unsteady flow hydraulic simulations on river channels and floodplains in a single river reach or a network of reaches (Brunner 2016; Dimitriadis et al. 2016).

HEC-RAS requires geometric data [e.g., river geometry, cross section profiles (XSs), Manning's coefficients, and hydraulic structures data] and flow data (flow regime and discharge data). For steady flow regime calculations, *HEC-RAS* uses the energy equation to compute the water surface level between river cross sections using an iterative procedure. To begin calculations, the program requires a starting water elevation or boundary condition at the downstream end of the river system for a subcritical flow regime or the upstream end for supercritical flow (Brunner 2016). Known WSE, normal depth (requires an energy slope for the river), critical depth, and rating curve are listed as available boundary condition options in *HEC-RAS* (Brunner 2016).

Creating the geometric data for hydraulic modeling is usually done in *HEC-GeoRAS*, which is an *ArcGIS* extension developed by the Environmental Systems Research Institute (ESRI). *HEC-GeoRAS* is capable of preprocessing geospatial data for creating a numerical model input file in the preferred format for the *HEC-RAS* model and postprocessing the results in *ArcGIS* (Ackerman 2012).

LITE Flood

The 100-year floodplain is a good starting point when identifying the risk of a large impact. However, emergency managers and policy makers want to consider smaller, more frequent floods. To recognize local flooding patterns and impacts in these occurrences, emergency planning requires flood inundation extents be determined for events with intervals of low, medium, to high risk, often masked by the strict one-size-fits-all approach of the 100-year floodplain.

The National Weather Service's Advanced Hydraulics Prediction Service (AHPS 2011) tool offers the capability to map flooding across a range of small-to-big severity for selected locations that is based solely on river stage elevation (NOAA 2011). AHPS uses a calibrated hydraulic model to determine an equivalent flood stage to a specific stream discharge based on an iterative trial and error approach (NOAA 2011). However, this approach is only applicable to a limited length of river reach that has an equal discharge throughout the river reach and thus does not simulate the entire river system.

Producing flood maps with more intervals (similar to AHPS) requires either new hydrologic and hydraulic studies or reconstruction of effective hydraulic models. Reconstruction of existing models has many operational difficulties. First, it is difficult to unify disparate hydraulic models, which have differing space and time scales, into a single file (Brody et al. 2013). When transforming models from older software versions like *HEC-RAS* into the newer *HEC-GeoRAS* version, the translation requires the arduous process of relating *HEC-RAS* river geometry representations to the more spatially representative GIS features. Secondly, model boundary conditions and hydrologic inputs will need to be realigned to a common point in time.

The LITE Flood is a simple and fast GIS-based approach for mapping smaller flood events that happen within the boundaries of a base flood (e.g., 100-year flood). The technique is applicable to areas where the water elevations of a base flood event have been identified through preliminary hydrologic and hydraulic studies such as those modeled by FEMA [Fig. 1(b)]. This technique obtains the ratio of the water surface drop between an upper and lower water surface boundary at a reference location and renders it to other locations to create the flood extent boundaries and the water depth maps of the corresponding events. Multifrequency depth grids are planned to be included in FEMA's RiskMap assessment product (FEMA 2010, 2013b).

LITE Flood requires a set of predefined cross section lines that are perpendicular to streamlines and cover the entire extent of the floodplain. FEMA DFIRMs supply such cross sections as part of their GIS data set. The cross sections are associated with WSE data and topography to determine upper (z_{max}) and lower (z_{min}) boundaries at each cross section.

The upper boundary is defined as the WSE of a large flood (e.g., $WSE_{100-year}$ or $WSE_{50-year}$ for approximation of a 25-year flood), and the lower boundary is the minimum elevation value. z_{min} can be one of the following: (1) the WSE of a small flood event (e.g., existing $WSE_{10-year}$ in a hydraulic model for prediction of a 25-year flood when adding more intervals between hydraulically modeled flood is desired); (2) the elevation of streambed; and (3) the WSE at the regular discharge. The best example of nonflooded water elevation is the light detection and ranging (LiDAR) driven DEM. Although some new laser perception devices used for LiDAR data collection are able to detect the bathymetry of shallow and clean water bodies (Kinzel et al. 2013; Fernandez-Dian et al. 2014; Kashani et al. 2015a), conventional techniques only map the surface of water because they cannot penetrate the water (NOAA 2012b; Kashani et al. 2015a).

An initial WSE during the flood of interest (z_{new}) at a reference location (kth cross section) is required to perform the interpolation calculations. The z_{new} can be one of the following: (1) high water marks (HWMs); (2) an equivalent flood stage for a desired flood event that could be obtained from rating curves that show the relationship between the discharge and WSE (such rating curves are generally available from USGS river stage stations); (3) flood elevation intervals between hydraulically modeled floods; and (4) a predicted flood stage for a storm or a specific flood stage that emergency responders are interested in mapping. Knowing $z_{new\,(k)}$, the z_{new} values are calculated by projecting the ratio of the water level drop (from z_{max}) in the difference of z_{max} and z_{min} to other cross sections [Eq. (1)]

$$z_{new(i)} = \begin{cases} z_{new(k)} & i = k \\ z_{max(i)} - c \times (z_{max(i)} - z_{min(i)}) & i \neq k \end{cases} \quad (1)$$

where $z_{new(i)}$ = data set of WSE for the intermediate flood event at cross sections $i = 1$ to n; $z_{new\,(k)}$ = known WSE at the kth cross section (reference); and c = interpolation coefficient that is calculated from Eq. (2) at the reference location (k)

$$c = \left(\frac{z_{max(k)} - z_{new(k)}}{z_{max(k)} - z_{min(k)} } \right) \quad (2)$$

Fig. 3 shows the flowchart of a systematic data processing for inundation mapping using the LITE Flood approach in *ArcGIS*. It takes the polylines of base flood elevations (BFE) and the raster data of DEM to determine the upper and lower boundaries. The calculated new elevations (z_{new}) on the cross section lines were used to interpolate a quasi-3D triangular irregular network (TIN) surface. The TIN was then converted into a raster to represent a continuous water surface. Lastly, the water surface raster was subtracted from the DEM to arrive at the final flood inundation area.

One of the limitations for the LITE flood model is that it does not consider flood protection facilities (e.g., levees, floodwalls, and gate valves). The flood protection facilities were designed based on large impact events (i.e., 100-year flood). The assumption of this technique is these facilities do not fail in flood events that do not reach the large impact event. Treating levees and flood walls as linear breaklines in the interpolation process can be difficult. Therefore, the resulting water surface map from the above procedure was clipped by the boundaries of the FEMA 100-year flood as the impact of those features on flooding have already been accounted for in the modeling.

Model Assessment

To assess the accuracy of the linear interpolation technique, its results were compared to *HEC-RAS* for the same corresponding flood event. Both graphics and statistics were used to evaluate the accuracy of the proposed method, in which the two geometric variables, WSE, and floodplain top width (TW) are subject to analysis. The measurements obtained from the *HEC-RAS* were assumed as reliable"observed values, and the results of LITE Flood were considered as estimated or predicted values.

The mean absolute error (MAE), mean bias error (MBE) and root-mean square error (RMSE) are commonly used error index statistics (Willmott and Matsuura 1995; Moriasi et al. 2007) and were used in the present analysis. The MAE was calculated by averaging the absolute magnitude of differences. If the sign of residuals is considered, the error index is called the MBE. MAE and MBE were formulated in Eqs. (3) and (4) as follows:

$$\text{MAE} = n^{-1} \sum_{i=1}^{n} |P_i - O_i| \quad (3)$$

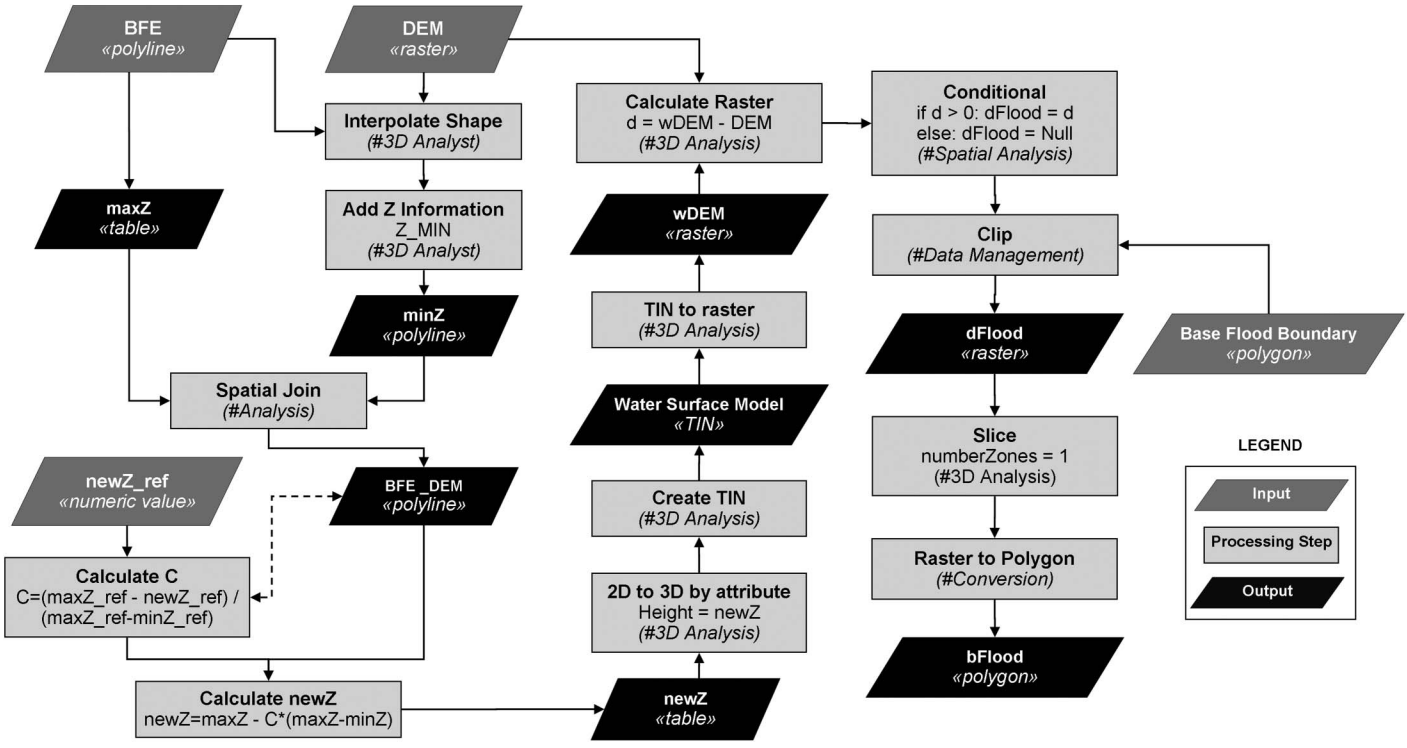

Fig. 3. Flowchart of inputs, outputs, and processing steps for the GIS-based LITE Flood modeling of a flood with a known reference WSE between upper and lower boundaries of BFE and LiDAR DEM; the angle quotation marks describe the format of input and outputs data, and the hashtag notations specify the required ESRI *ArcGIS* extensions for data processing

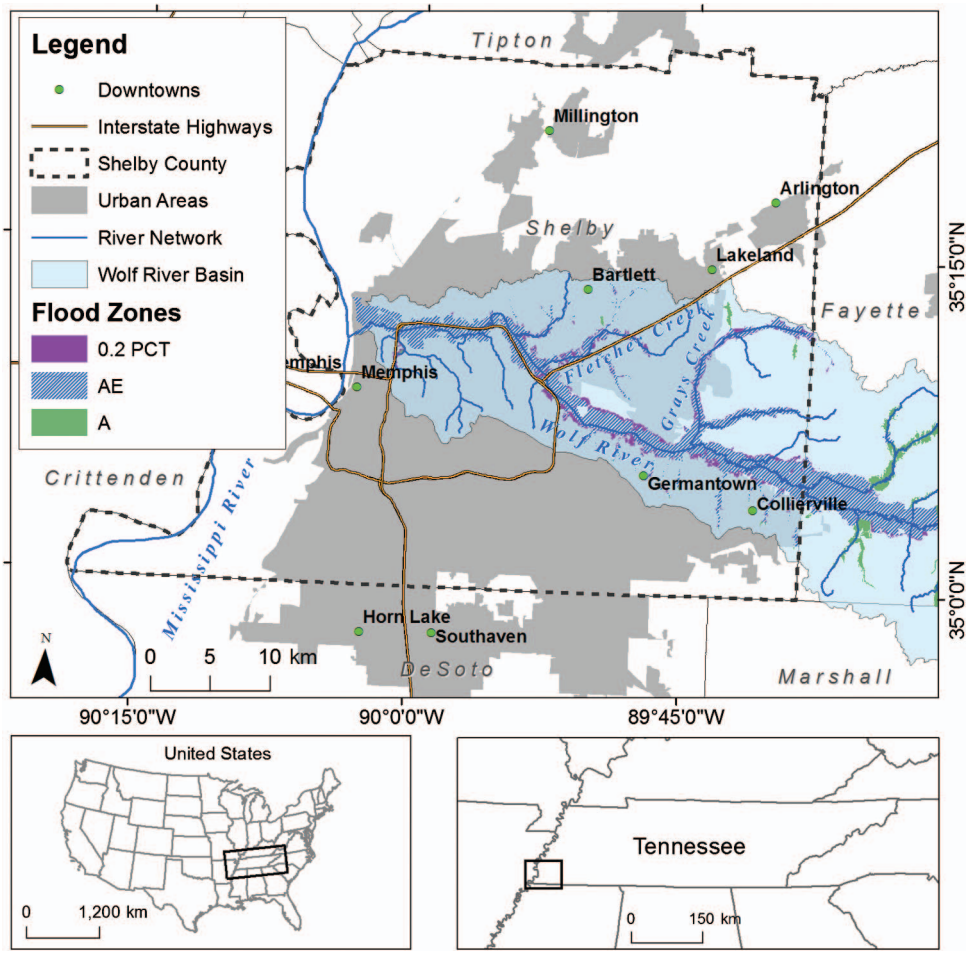

Fig. 4. (Color) Study area, which is the portion of Wolf River basin in Shelby County, Tennessee, and FEMA's 100-year (Zones AE and A; Zone A is equivalent to Zone AE, but the mapping of Zone A is done using approximation techniques rather than hydraulic modeling) and 500-year (0.2 PCT) flood inundation extents (highway data from Esri, Tele Atlas North America; map data from Esri, National Atlas of the United States, United States Geological Survey, Department of Commerce, Census Bureau—Geography Division)

Table 1. Summary of Geometry and Flow Data Imported from the *HEC-2* Models

Attribute	Wolf River	Fletcher Creek	Grays Creek
Reach length	From the confluence with Mississippi River to 54.4 km upstream	From the confluence with Wolf River to approximately 17.1 km upstream	From the confluence with Wolf River to approximately 12.7 km upstream
Model original format	*HEC-2*	*HEC-2*	*HEC-2*
Effective date	December 2, 1994	December 15, 2004	May 24, 1999
Number of cross sections	132	73	57
Number of bridges	23	12	3
Channel Manning's n-values	0.045–0.07	0.04–0.06	0.025–0.05
Average discharge (m^3/s)			
$Q_{10\text{-year}}$	537	149	183
$Q_{50\text{-year}}$	771	187	233
$Q_{100\text{-year}}$	906	204	254
$Q_{500\text{-year}}$	1,320	245	296
Boundary condition	Normal depth: $S = 0.00009$, known WSE (m): $WSE_{100\text{-year}} = 71.02$	Known WSE (m): $WSE_{10\text{-year}} = 74.02$, $WSE_{50\text{-year}} = 74.27$, $WSE_{100\text{-year}} = 74.47$, $WSE_{500\text{-year}} = 75.28$	Known WSE (m): $WSE_{10\text{-year}} = 82.14$, $WSE_{50\text{-year}} = 82.84$, $WSE_{100\text{-year}} = 83.27$, $WSE_{500\text{-year}} = 83.88$

$$\text{MBE} = n^{-1}\sum_{i=1}^{n}(P_i - O_i) \quad (4)$$

where P_i = predicted value at the ith cross section; O_i = pairwise matching observed value; and n = number of cross sections.

The RMSE is the variance of difference between the predicted and observed values. To generate a dimensionless error index, Singh et al. (2005) introduced the RMSE observations standard deviation ratio (RSR), as formulated in Eq. (5), which was calculated as the ratio of RMSE and the standard deviation of

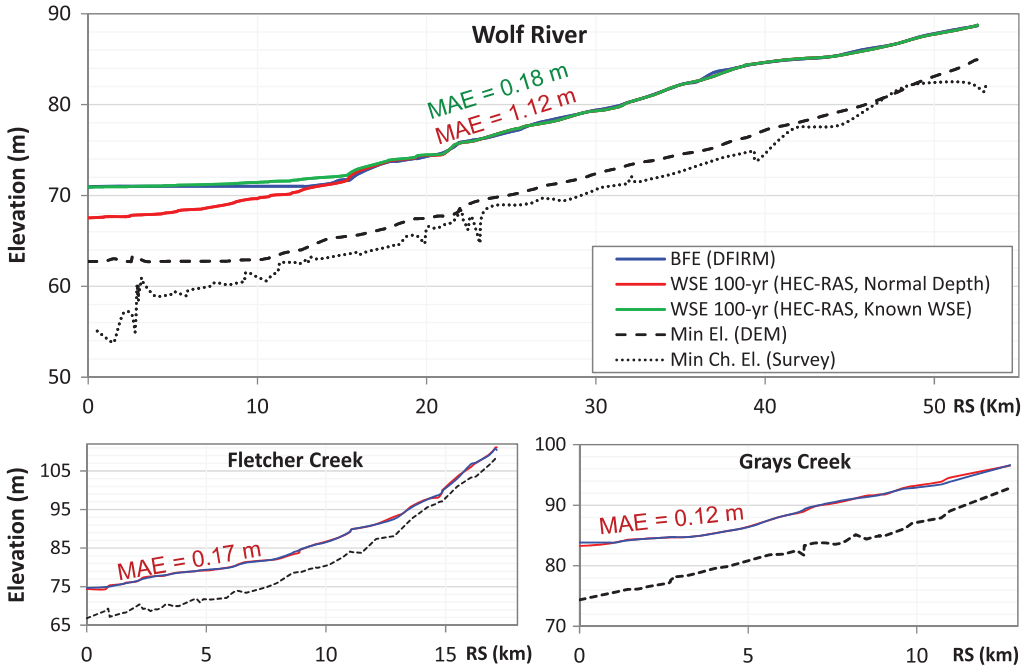

Fig. 5. (Color) WSE prediction for a 100-year flood calculated through *HEC-RAS* model with different boundary conditions (known WSE and normal depth) in comparison to the BFE in FEMA's DFIRM; the dotted line presents the channel bottom elevation, and MAE is the average of the absolute differences between the WSE and BFE at XSs

observations. According to Moriasi et al. (2007), very good to satisfactory values of RSR fall in range of 0.0–0.7

$$\text{RSR} = \frac{\text{RMSE}}{\text{Standard deviation}_{(O_i)}} = \frac{\sqrt{n^{-1}\sum_{i=1}^{n}(P_i - O_i)^2}}{\sqrt{n^{-1}\sum_{i=1}^{n}(O_i - \bar{O})^2}} \quad (5)$$

Data Set

The study area is a portion of the Wolf River and its two main tributaries (Fletcher Creek and Grays Creek) that are located within the borders of Shelby County, Tennessee (Fig. 4). In total, the Wolf River is 138 km long with a 2,121 km^2 watershed of which 25% resides within Shelby County's border (future discussion will pertain to that portion of the watershed in Shelby County). The Wolf River drains about one-fourth of the Shelby County area as it flows from east to west before its confluence with the Mississippi River just north of downtown Memphis. Fletcher Creek and Grays Creek have 83 and 148 km^2 of contributing total basin area, respectively. Topography within the Wolf River watershed ranges from 60 to 130 m above mean sea level with the lowest elevations expectedly located near the confluence of the Wolf River with the

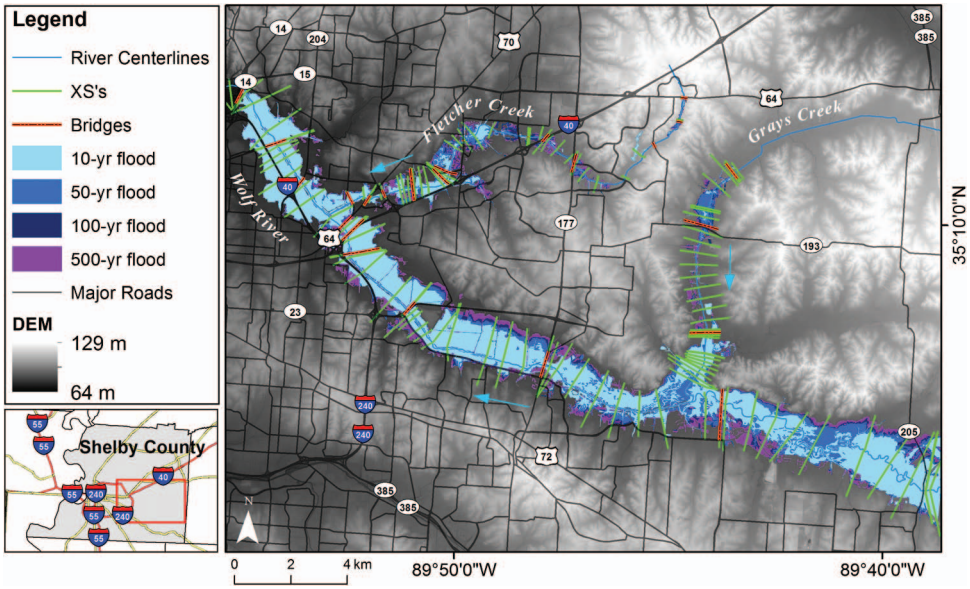

Fig. 6. (Color) 10-, 50-, 100-, and 500-year flood extents modeled in *HEC-RAS*, the rivers network, and the georeferenced XSs and bridges; the base image is the LiDAR DEM, in which brighter color shows higher elevations (highway data from Esri, Tele Atlas North America; county line data from Esri, StoryMaps)

Table 2. List of Reference Points with Known Water Surafce Elevation for 50- and 10-Year Floods

Reference name	Stream name	River station (km)	z_{new} (m)	
			50-year	10-year
R_D	Wolf River	16.0	72.32	71.85
R_M	Wolf River	31.3	79.47	78.81
R_U	Wolf River	41.3	84.62	83.78

Mississippi River. The area receives an average precipitation of 130 cm per year, with precipitation more common from March to May and November to December (NOAA 2012a).

The upstream section of the Wolf River basin east of Grays Creek consists of a mixture of forest, wetland, and agricultural areas, whereas the lower section is dominated by urban development. To reduce flooding impacts, the lower 35.4 km of the river was channelized in 1964 by the USACE (1995). As a result of the

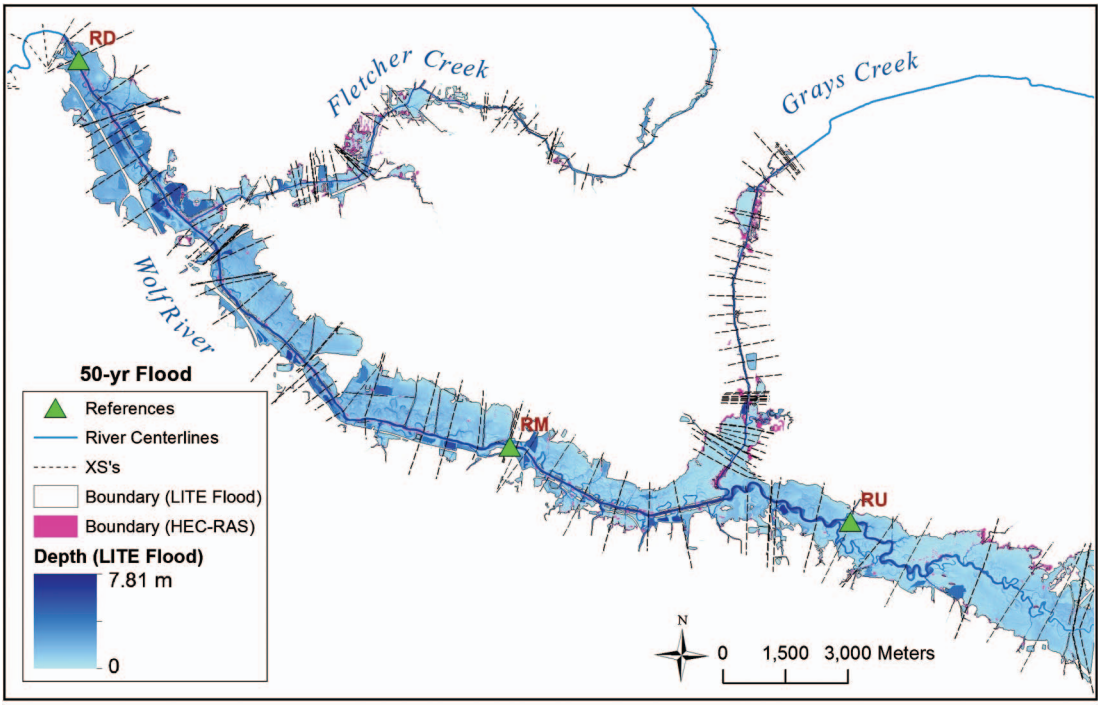

(a)

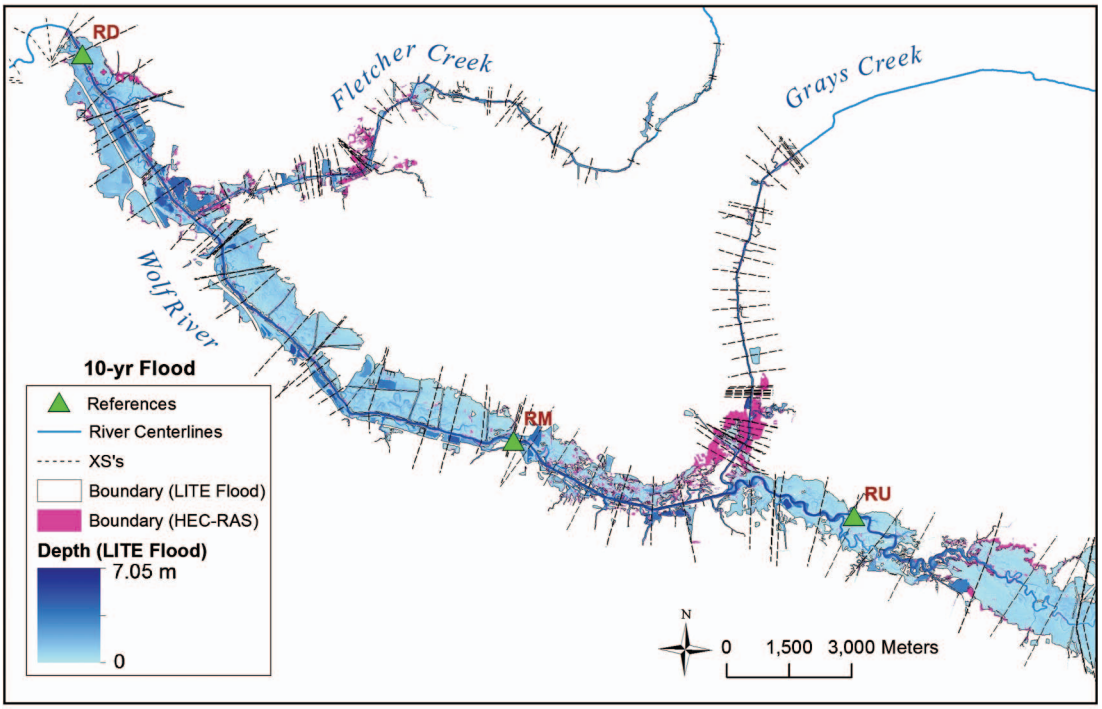

(b)

Fig. 7. (Color) Floodplain delineation and inundation depth using LITE Flood: (a) 50-year; (b) 10-year floods

channelization, the straighter, steeper, deeper, wider, and smoother channels produce a more flashy response to storm events. Additionally, development has encroached closer to the Wolf River floodway and has thus increased the potential for property damage during flood events (Van Arsdale et al. 2003; Poff et al. 1997; USACE 1995). Most recently, severe storms in the Memphis area in May 2010 dumped as much as 25–38 cm in 2 days (NOAA 2010). This resulted in substantial flooding that damaged infrastructure and properties along the Wolf River and its tributaries (TEMA 2010).

The FEMA (2013a) DFIRM, 47157C (effective date September 28, 2007), is the most current flood map for Shelby County. The geodetic coordinate system is Tennessee State Plane, referenced to Geodetic Reference System 80 (GRS 80) datum, and the vertical reference is North American Vertical Datum of 1988 (NAVD88). Accompanying the DFIRM are a number of GIS data sets including floodway information, the 100- and 500-year flood hazard zones (Fig. 4), and the BFE (water elevation transects for the 100-year flood). The DFIRM data set was developed by estimating floodwater elevations through hydraulic modeling of river reaches in the area.

There are three topographic data sets for the study area: the USGS 30- and 10-meter DEM and a more recent data set of 1-m resolution rasterized LiDAR DEM. The USGS DEM data was used in developing the FEMA (2013a) DFIRM models. The LiDAR data, acquired by USGS and National Geospatial Technical Operations Center (NGTOC) between December 2011 and January 2012, is used in our study to map the lateral flood extents simulated by hydraulic models. These data are important in LITE Flood analysis because the objective is to approximate the WSE for smaller storm events using the water surface of a large flood with topography as the primary contributing parameters.

Results and Discussion

The following subsections outline and discuss the data preparation and results of this study. First, the approach for *HEC-RAS* modeling is discussed. Then the results of the calibrated model in producing flood frequency maps is argued. Next, the LITE Flood is used to generate inundation maps of the same flood event modeled in *HEC-RAS*. Finally, the accuracy of the LITE Flood is assessed by comparing the results from both techniques.

Hydraulic Simulation

Building the Model

Keeping the original geometric and flow settings, the hydraulic models developed by FEMA's mapping partners for producing the DFIRM were used in this study. All three river reaches were modeled using *HEC-2*, the older generation of *HEC-RAS*, which in comparison to its current version, has less computational features and lacks the georeferencing capability of streams and cross sections. To convert the *HEC-2* data to a *HEC-RAS* model, it was required to define the location of geometric features; however, there is no direct and defined approach for achieving this. The most favorable situation is when the cross sections are digitized in the DIFRM data set or their paper maps are available. For this study, the paper maps were not available, and there was no consistency in terms of naming convention nor the number of cross sections in *HEC-2* and the cross sections included in DFIRM. Therefore, the river stations (RS) or the distances from the most downstream point on the river, which identically exists in both versions, must be used to locate the position of cross sections along the river. To georeference the *HEC-2* for the Wolf River, a new geometry of stream centerlines were populated and stationed in *HEC-GeoRAS*. The location of fixed benchmarks (e.g., bridges) in *HEC-2* were matched against their location using *ArcGIS* imagery basemaps to create the best match for the river station values. The shortening or lengthening of river centerline segments between the benchmarks was required to match the stationing in the reproduced model to the stationing in the existing models. As the new river geometry was populated in *HEC-GeoRAS*, the existing geometry data (including cross sections and bridges from *HEC-2* data) was imported on the georeferenced river centerline. This process ends up with cross sections that are not georeferenced yet but they are perpendicular to the river centerlines at the affiliated river stations. The georeferencing of the perpendicular cross sections was finalized by checking and repositioning the cross section vertices to create a length consistency between with *HEC-2* and GIS cutlines in *HEC-RAS*. The display ratio of cutline length to cross section length command in *HEC-RAS* was very helpful for this task.

Input Data for *HEC-RAS* Model

Table 1 summarizes the geometric data (i.e., streams, XSs, range of Manning's coefficients in river channels, and hydraulic structures data) and the flow data (e.g., discharge data and boundary

Table 3. WSE and TW Prediction Error Statistics Resulting from the LITE Flood Approach When Using Different Lower Boundaries Elevations and Reference Stations

				Error statistics					
				z_{min} (DEM)			z_{min} (SUR)		
Flood severity	Measurement	Error index	Unit	R_D	R_M	R_U	R_D	R_M	R_U
50-year	WSE	MBE	m	0.07	−0.12	−0.06	0.08	−0.09	−0.10
		MAE	m	0.09	0.13	0.10	0.10	0.11	0.12
		RSR	—	0.02	0.02	0.02	0.02	0.02	0.02
	TW	MBE	m	34	−77	−43	41	−67	−69
		MAE	m	57	83	65	57	76	78
		RSR	—	0.17	0.24	0.2	0.16	0.22	0.22
10-year	WSE	MBE	m	0.17	−0.20	−0.26	0.21	−0.14	−0.39
		MAE	m	0.25	0.27	0.31	0.26	0.23	0.41
		RSR	—	0.04	0.05	0.06	0.05	0.04	0.07
	TW	MBE	m	40	−72	−87	53	−62	−146
		MAE	m	68	88	97	66	75	146
		RSR	—	0.26	0.39	0.41	0.26	0.31	0.55

condition) used in hydraulic modeling. *HEC-RAS* uses a 1D energy equation (for steady flow) to compute the water surface level between river XSs (Brunner 2016). A known WSE boundary condition was used for Fletcher Creek and Grays Creek to account for backwater conditions from the Wolf River. However, hydraulic simulation of the Wolf River was performed using two boundary conditions for model calibration purposes: (1) the normal depth that is included in the original *HEC-2* model, and (2) a known WSE that is obtained from a BFE cross section at the confluence of the Wolf River with Mississippi River.

Model Calibration

The hydraulic simulation was performed under a subcritical steady flow regime and with water elevations calculated at each cross section for each reach. The calculated WSE for 100-year flood ($WSE_{100\text{-year}}$) were compared to BFE in DFRIM data sets (Fig. 5).

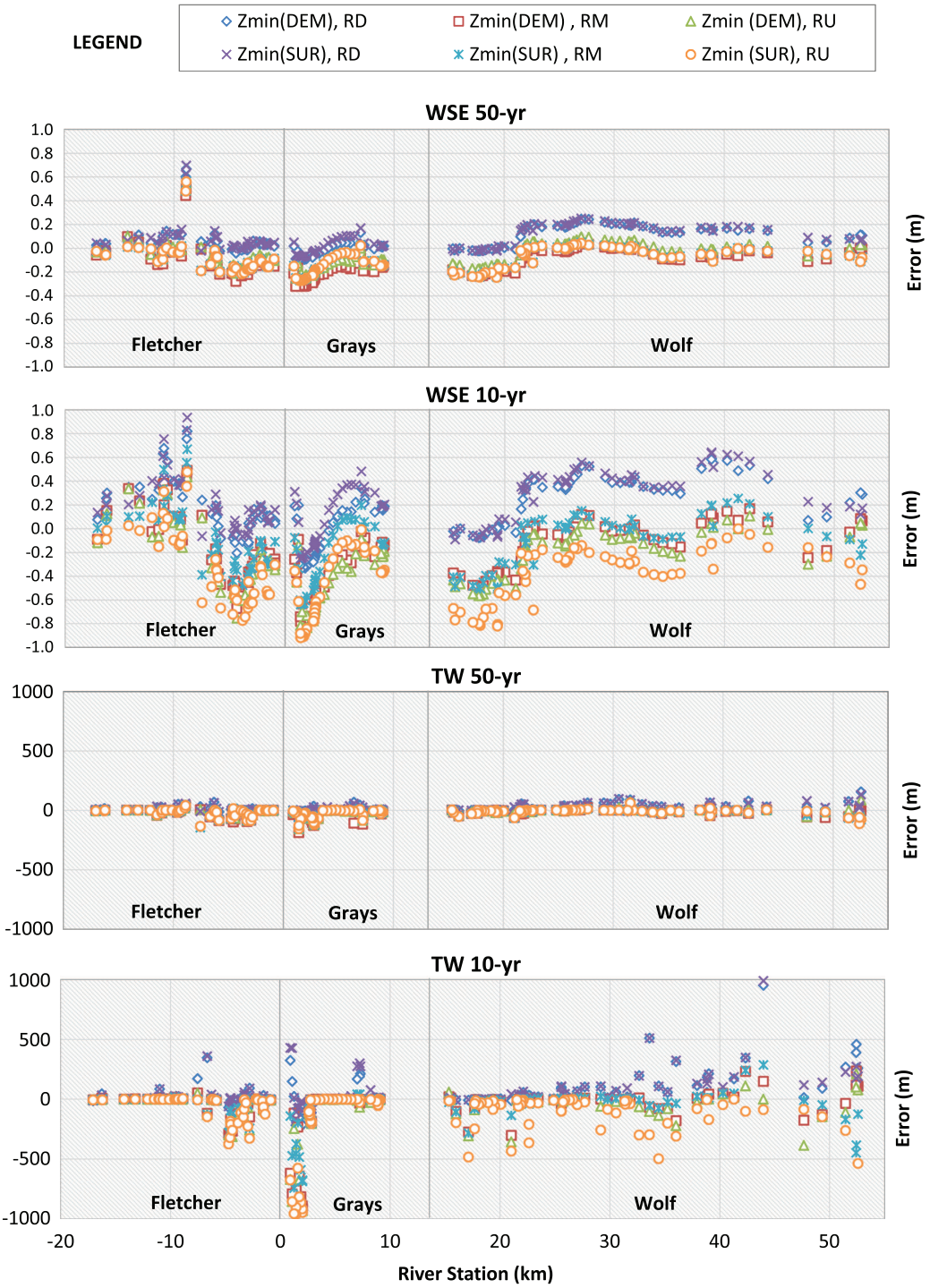

Fig. 8. (Color) Difference between predicted WSE and inundation TW by LITE Flood and the observed values resulting from *HEC-RAS* for 50- and 10-year flood events; interpolation is performed using upper boundary 100-year WSE and two lower boundaries (DEM and SUR) with three references at R_D, R_M and R_U; each diagram consists of three sections for each river reach; the negative river stationing has been used to show all reaches in one plot (unlike Grays Creek and Wolf River, Fletcher Creek is shown from upstream to downstream and with negative signs)

Fig. 5 shows that the hydraulic models for Fletcher and Grays Creek are capable of reproducing the FEMA data with MAE of 0.12 and 0.17 m (error statistics are discussed later). However, using the normal depth boundary condition (applied at the mouth of the river) causes significant error in the downstream section of the Wolf River, where *HEC-RAS* initiates the WSE calculations. The $WSE_{100\text{-year}}$ and BFE eventually converge 15 km upstream from where the boundary condition is applied. The other boundary condition option is setting a WSE at known location. Setting the known WSE as the boundary condition improves the correspondence of WSE100-year and BFE, but WSEs are not available for any other flood events other than the 100-year flood. Therefore, the normal depth was considered to be the best boundary condition; however, the 15 km downstream section of Wolf River had to be excluded from further analysis.

Multifrequency Flood Mapping by *HEC-RAS*

With the hydraulic model calibrated, the hydrologic data for a 10-, 50-, and 500-year flood, as well as a 100-year flood, were simulated in *HEC-RAS*, and the WSE of multifrequency floods was calculated. The hydrologic inputs for these scenarios were included in the original *HEC-2* models. The resulting flood inundation extents derived from *HEC-GeoRAS* are shown in Fig. 6.

Inundation Mapping by LITE Flood

Flood inundation mapping of intermediate storms (with 50 years and 10 years return chance) was performed using the LITE Flood approach. The XS lines from hydraulic modeling were used as input cross sections, where $WSE_{100\text{-year}}$ on XSs were appointed as the upper boundary. Two lower boundaries were obtained from two sources: (1) $z_{\min(\mathrm{DEM})}$ that depicts the water surface of streams during a nonflooded situation as obtained from the minimum LiDAR elevation value in the stream at each XS; and (2) $z_{\min(\mathrm{SUR})}$ that is the surveyed cannel bottom measurements that were included in the *HEC-2* models. To perform the GIS approach, a reference $z_{\mathrm{new}(k)}$ value is required to initiate the projection of the flood stage from the reference location to the entire river network. One known WSE value is enough for processing, but does placement of the reference location impact the results? To determine if placement of the reference point is independent of location along the stream, three reference locations (Fig. 8) were chosen for testing: downstream (R_D), middle (R_M), and upstream (R_U) of the Wolf River. The R_D and R_M locations coincide with two USGS gauging stations on the Wolf River (at river stations 16.0 and 31.3 km), and R_U is a cross section at 41.3 km (Table 2). Fig. 7 presents the water depths and delineations of inundated areas for 50- and 10-year floods in the context of the upper 100-year boundary and lower DEM boundary.

Table 4. WSE and TW Prediction Error Statistics Resulted from LITE Flood Approach When Using Different Lower Boundaries Elevations and Average of Reference Stations

				Error statistics	
Flood severity	Measurement	Error index	Unit	$z_{\min}$ (DEM) (average)	$z_{\min}$ (SUR) (average)
50-year	WSE	MBE	m	−0.04	0.00
		MAE	m	0.09	0.09
		RSR	—	0.02	0.02
	TW	MBE	m	−30	−6
		MAE	m	59	54
		RSR	—	0.18	0.15
10-year	WSE	MBE	m	−0.10	−0.10
		MAE	m	0.23	0.22
		RSR	—	0.04	0.04
	TW	MBE	m	−37	−51
		MAE	m	71	68
		RSR	—	0.29	0.28
10-year (with 50-year flood upper boundary)	WSE	MBE	m	−0.06	−0.07
		MAE	m	0.15	0.15
		RSR	—	0.03	0.03
	TW	MBE	m	−23	−28
		MAE	m	45	42
		RSR	—	0.19	0.16

Model Assessment

Table 3 summarizes the error index statistics for the LITE Flood calculation in the study area. Fig. 8 displays the prediction error for WSE and TW for 50- and 10-year floods analyzed at the cross sections. As shown in Fig. 8, the WSE prediction error for the 50-year flood ranges between −0.35 and 0.25 m (except for two cross sections on the Fletcher Creek). The error function has a similar trend as it moves up or down based on the location of the reference XS. As expected, the error is zero at the reference location. As shown in Table 3, $WSE_{50\text{-year}}$ prediction error (MAE) ranges between 0.06 and 0.12 m, in which the calculations based on R_D are overestimating (positive MBE), and calculations with R_M and R_U are underestimating (negative MBE). The predictions mostly underestimate the values when R_M and R_U are used, perhaps because LITE flood cannot hydraulically model the backwater from other tributaries when a reference station at the upper section of the river is selected. The biggest discrepancy between *HEC-RAS* and LITE Flood occurred at the beginning of Grays and Fletcher Creeks (Fig. 8), which can be related to the lack of backwater calculations in LITE Flood. Overall, the WSE predictions have an acceptable accuracy with an RSR of nearly 0.02. The MAE and RSR indexes for calculations with $Z_{\min}$ values extracted from DEM and surveyed cannel bottom measurements (SUR) are similar, implying that calculation using both interpolation lower boundaries produces similar results.

The biggest prediction error for $WSE_{50\text{-year}}$ (0.70 m) occurs at two cross sections behind a bridge at the 8.9-km river length of Fletcher Creek. The reason is that the 100-year discharge passing through the bridge is simulated in *HEC-RAS* as a high flow situation—high flow occurs when the stage reaches the lowest structural horizontal support (or chord) of the bridge deck (Brunner 2016). However, the discharge of the 50-year flood occurs as a low flow condition. Because the LITE Flood is not a hydraulic simulation, it simply rescales the WSE resulting from the larger flood supposing that it has a comparable but abated hydraulic behavior to

Table 5. Inclusion and Exlusion Errors in Flood Zone Classification Using LITE Flood Based on the Parcel Land Uses

	Error of inclusion (false alarm)		Error of exclusion (fail to alarm)	
Parcel land use	50-year	10-year	50-year	10-year
Single family	12	6	108	15
Duplex	—	—	4	5
Vacant land	3	3	4	4
Service GRG	—	—	1	—
Condo unit	—	1	—	4
Cell tower site	—	—	—	1
LOFT manufacture	—	—	—	1
PUD-detached	7	5	—	—
SHP-CTR-STRP	1	—	—	—
Sum	23	15	117	30

Note: GRG = garage; PUD = planned unit development; SHP-CTR-STRP = shopping center–strip center.

the large flood; therefore, it overestimates the WSE of the smaller event while it has a low flow condition at the bridge. Similarly, the approach will not have the capability to locate hydraulic jumps when the channel warrants a mixed flow regime (Brunner 2016).

For $TW_{50\text{-year}}$ predictions, the MAE ranges from 57 to 83 m. Similar to the WSE, the TWs are overestimated or underestimated based on the selection of the reference with an acceptable prediction error (RSR approximately 0.20) (Table 3). Owing to a flat, low-lying topography in the floodplain, even small changes in WSE cause significant change in TW. As shown in Fig. 8, the prediction error is higher for XSs in upstream sections of the Wolf River and in downstream sections of Grays Creek where the floodplain is flat and the TWs are wider. This means the estimation error depends on the length of TWs, and thus is larger for wider TWs.

The response of the 10-year flood is congruous with the 50-year flood with regard to the overestimation and underestimation of WSE based on the reference location, and it follows a similar pattern for TW prediction error across the river length. However, the error grows and its range expands for the smaller flood (Fig. 8). On average, the MAE changes from 0.10 to 0.20 m, with the highest error (MAE at 0.40 m) for $z_{\min}(\text{SUR})$ at reference R_U. The RSR increases by 2.5 times but still represents a good estimation for $WSE_{10\text{-year}}$. For TW prediction, the MAE ranges from 66 to 146 m, and RSR ranges from 0.26 to 0.55. The prediction can be considered satisfactorily accurate. This implies that the prediction error increases as the difference between storm event frequencies increase in relation to the reference event (e.g., estimating 10-year flood event form 100-year storm).

The predictions are overestimated for R_D, and underestimated for R_M and R_U stations, and the results could be improved by averaging the different water surfaces obtained for multiple references. Averaging the water surfaces could be achieved by averaging the interpolation coefficient (c) for all references. Table 4 shows the summary of statistics for WSE and TW prediction errors using the average c-value for reference locations. The results improved significantly for WSE predictions (MAEs of approximately 0.10 and 0.20 m for 50- and 10-year floods, respectively). In addition, TW prediction was enhanced for both floods as indicated by reduction in the RSR from 0.24 to 0.18 and 0.55 to 0.28 (for the largest prediction error) for 50- and 10-year, respectively.

Flood Zone Classification Errors

Fig. 7 shows that two mapping techniques do not return full overlapping results. Comparing the results from *HEC-RAS* and LITE Flood, two types of misclassification may happen: (1) false alarm or inclusion error occurs for areas that are mistakenly mapped in the flood zone in LITE Flood, but are not in *HEC-RAS* flood zones; and (2) fail to alarm or exclusion error occurs when LITE Flood fails to map the flood zone. The errors are also called Error Types I and II, respectively (Peck and Devore 2011). Models with negative MBE

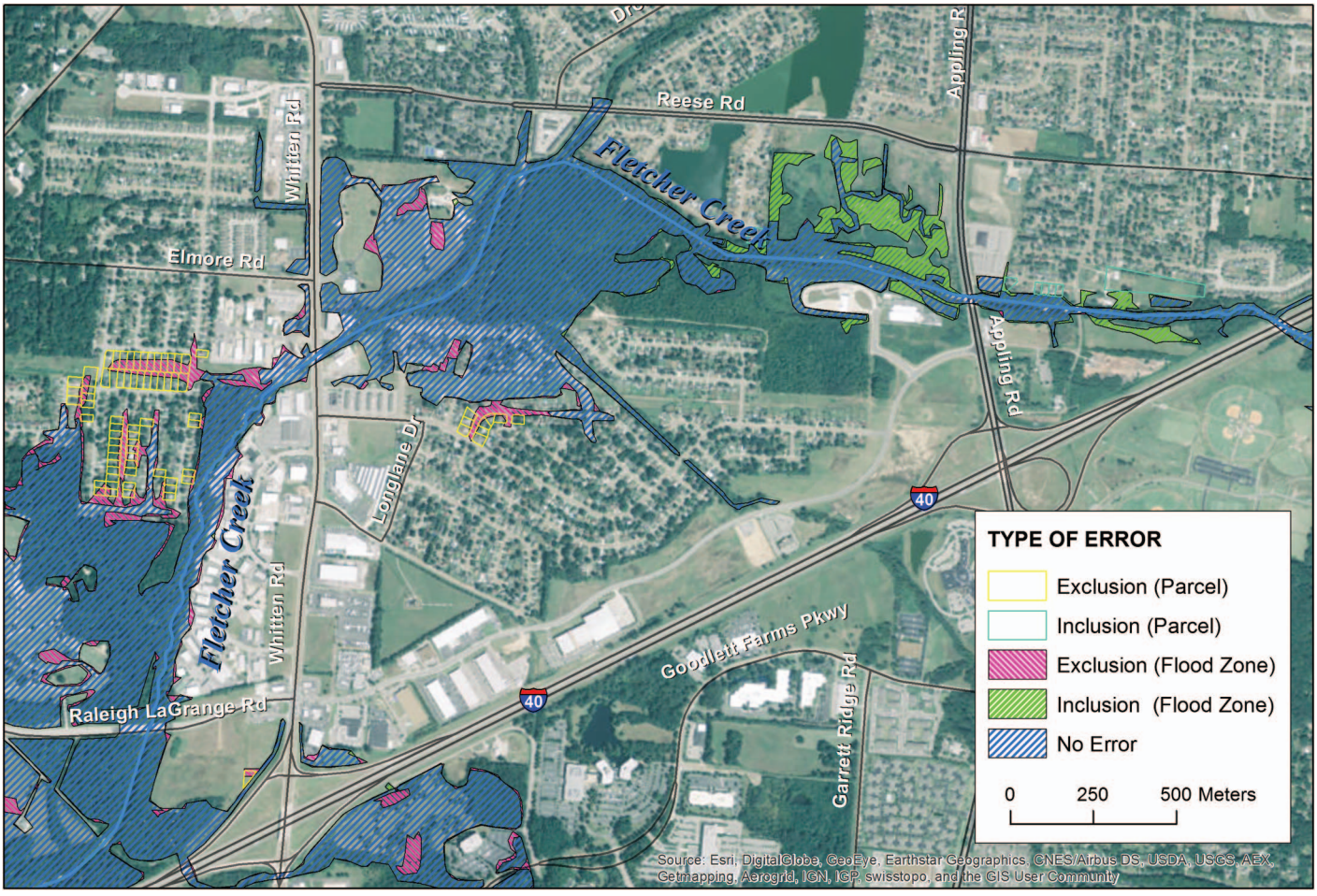

Fig. 9. (Color) Examples of misclassifications for the 50-year flood scenario using LITE Flood compared to *HEC-RAS*; the basemap is Esri's world imagery (map data from Esri, DigitalGlobe, GeoEye, Earthstar Geographics, CNES/Airbus DS, USDA, USGS, AEX, Getmapping, Aerogrid, IGN, IGP, swisstopo, and the GIS User Community)

(Table 4) underestimate the flood magnitude and produce results with more error of exclusion; however, models with positive MBE generate more error of inclusion.

The 2012 land parcel data set of the Shelby County was used to represent the flood alarm errors. The 50- and 10-year flood maps from LITE Flood was produced with a LiDAR DEM lower boundary, and averaged upper boundaries (three reference stations) (Table 4) were compared to the corresponding *HEC-RAS* results. For the entire study area, 1,875 parcels intersect or are within the 100-year flood plain, based on *HEC-RAS* simulations. The number of parcels impacted by 50- and 10-year flood events are 1,197 and 871, respectively (in *HEC-RAS*). Table 5 shows the number of misclassified parcels with inclusion and exclusion errors. Approximately 11% of the parcels have one form of inclusion or exclusion errors for the 50-year flood. This error is approximately 5% for a 10-year flood scenario. Fig. 9 presents examples of errors in parcel classification for the 50-year flood scenario using LITE Flood compared to *HEC-RAS* for a section of Fletcher Creek.

Conclusions

In this study, LITE Flood, a simple GIS-based flood mapping approach, was used and analyzed. The modeling was based on interpolation of intermediate flooding scenarios between an upper and lower boundary of water surfaces and is applicable in the areas where a large flood event has been modeled through preliminary hydrologic and hydraulic studies such as the counties with FEMA DIRFM data. The LITE Flood approach was evaluated by comparing its results to results from the standard numerical hydraulic model, *HEC-RAS*.

This study presented the strengths and weaknesses of the approach. The interpolation approach produced results with good to acceptable accuracy for the 50- and 10-year in the case study of Wolf River basin. The overall performance of the model could be improved by coupling more reference points into the analysis. However, the model has better performance when the upper and the intermediate floods are closer in terms of severity. In addition, the approach should be handled with more care if special attention to bridges is required or in areas where mixed flow simulation is performed in preliminary hydraulic modeling.

A primary concerns in using airborne LiDAR data for hydraulic modeling is that most of them do not include bathymetric data, so other measurements are required to derive bed elevation data. Updating the existing hydraulic models using the LiDAR-based DEM is usually an arduous procedure by extracting the overbank elevation data from DEM and *burning in* the channel geometry from other data sources. However, a good advantage of LITE Flood is that it works with different lower water surface boundaries, including the channel bed elevation at zero discharge and also the conventional LiDAR data that, when captured, may reflect a normal in-bank discharge.

The other asset of this approach is that it considers flood severity on scale of river stage elevation at the reference locations and predicts a similar flood across the floodplain. Flood severity based on percentage of annual flooding chance is best for determining design floods, but developing it using flood-stage levels provides a more simplified approach with relatively tolerable error. In addition, this approach is able to produce the flood inundation depth grids that have been considered a useful flood risk assessment tool and have been planned to be included in new flood risk products.

LITE Flood can be a useful feature for web GIS applications (Fu and Sun 2010) that require quick, on-the-fly processing and visualization of inundation maps. The multifrequency inundation map could be incorporated into animated maps that present gradual changes of floodplain extents and the local flooding patterns in respect to continuous fluctuations in water level. LITE Flood could effectively be used for adding intermediate flood events between the hydraulically modeled floods such as the *HEC-RAS* model and AHPS tools. Using LITE Flood eliminates a need for conducting new studies (e.g., flood frequency analysis, regional regression, and hydrologic modeling) that would require an estimate of the discharge of the intermediate flood (required at each flow data input location) and reiterating the hydraulic modeling with the intermediate discharge. In addition, it bypasses the trial-and-error approach for finding the flood stage in AHPS models.

The choice of approach for flood inundation mapping strongly depends on the scope and the scale of a study and the tolerable error. LITE Flood is not meant to do hydraulic modeling and does not consider the soil's saturation. LITE Flood is not suited for serious planning and design purposes that usually consider the large impact 100-year flood. Using simpler techniques by limiting the number of contributing parameters will sacrifice a part of accuracy. However, the present approach is developed based on the widely available and commonly used *ArcGIS*, could be quickly constructed, and could be effectively used for swift assessment of smaller floods at large scales, especially when developing sophisticated hydraulic models or the setup of existing models is not feasible because of shortage in time, data, personnel, and budget.

Acknowledgments

This research was conducted in the Center for Applied Earth Science and Engineering Research (CAESER) (www.memphis.edu/caeser), and was presented to the University of Memphis (UoM) at Memphis, Tennessee, in partial fulfillment of the requirements for the degree of Master of Science (Javadnejad 2013), under supervision of Dr. Brian Waldron (Department of Civil Engineering, UoM). The funding for this study was provided as a part of the Phase II project for GIS development of the Memphis/Shelby County Urban Area Security Initiative (UASI) through the contract with the Department of Homeland Security (DHS) (2012). We would like to thank the Hydrologic Engineering Center of the USACE in the Memphis District, particularly Mr. Brian Hall, for sharing their professional experience in hydraulic modeling and providing a quota of the required data sets. We also thank Dr. Dorian Burnette (Department of Earth Sciences, UoM) and the two anonymous reviewers for their valuable comments and suggestions on improving the quality of this paper.

References

Ackerman, C. T. (2012). "HEC-GeoRAS: GIS tools for support of HEC-RAS using ArcGIS 10 user's manual." *Rep. No. CPD-83*, U.S. Army Corps of Engineers, Hydrologic Engineering Center, Davis, CA.

AHPS (Advanced Hydraulics Prediction Service). (2011). "National oceanic and atmospheric administration (NOAA)." ⟨http://water.weather.gov/ahps/inundation.php⟩ (Mar. 14, 2011).

ArcGIS [Computer software]. Esri, Redlands, CA.

Brody, S. D., Blessing, R., Sebastian, A., and Bedient, P. (2013). "Delineating the reality of flood risk and loss in southeast, Texas." *J. Nat. Hazards Rev.*, 10.1061/(ASCE)NH.1527-6996.0000091, 89–97.

Brunner, G. W. (2016). "HEC-RAS hydraulic reference manual, version 5.0." *Rep. No. CPD-69*, U.S. Army Corps of Engineers, Hydrologic Engineering Center, Davis, CA.

Dickerson, T. A. (2007). "Development and evaluation of the profile synthesis method for approximate floodplain redelineation." M.S. thesis, Virginia Polytechnic Institute and State Univ., Blacksburg, VA.

Dimitriadis, P., et al. (2016). "Comparative evaluation of 1D and quasi-2D hydraulic models based on benchmark and real-world applications for uncertainty assessment in flood mapping." *J. Hydrol.*, 534, 478–492.

EXCIMAP (European Exchange Circle on Flood Mapping). (2007). *Handbook on good practices for flood mapping in Europe*, European Environment Agency, Copenhagen, Denmark.
FEMA. (2002). "Guidelines and specifications for flood hazard mapping partners appendix C: Guidance for riverine flooding analyses and mapping." ⟨https://www.fema.gov/media-library/assets/documents/13948⟩ (May 30, 2016).
FEMA. (2005). "Floodplain management requirements: A study guide and desk reference for local officials." ⟨http://www.fema.gov/media-library/assets/documents/6417?id=2165⟩ (Dec. 5, 2006).
FEMA. (2010). "Risk assessment product: Multi-frequency depth grids." ⟨http://www.fema.gov/media-library/assets/documents/19041⟩ (May 1, 2014).
FEMA. (2013a). "Digital flood insurance rate map database, Shelby County (and incorporated areas) (CD-ROM)." Washington, DC.
FEMA. (2013b). "FEMA's risk mapping, assessment, and planning (risk MAP) fiscal year 2012 report to congress." ⟨https://www.fema.gov/media-library/assets/documents/26717⟩ (May 1, 2014).
FEMA. (2015a). "Draft federal flood risk management standard implementing guidelines." ⟨https://www.fema.gov/media-library/assets/documents/101761⟩ (Jan. 30, 2015).
FEMA. (2015b). "The National Flood Insurance Program (NFIP), flood hazard mapping, map modernization." ⟨http://www.fema.gov/national-flood-insurance-program-flood-hazard-mapping/map-modernization⟩ (Jun. 2, 2015).
FEMA. (2016). "The National Flood Insurance Program (NFIP), media resources." ⟨http://www.floodsmart.gov/floodsmart/pages/media_resources/stats.jsp⟩ (May 19, 2016).
Fernandez-Diaz, J. C., et al. (2014). "Early results of simultaneous terrain and shallow water bathymetry mapping using a single-wavelength airborne LiDAR sensor." *IEEE J. Sel. Top. Appl. Earth Observ. Remote Sens.*, 7(2), 623–635.
Fisher, R. P., and Myers, B. A. (2011). "Free and simple GIS as appropriate for health mapping in a low resource setting: A case study in eastern Indonesia." *Int. J. Health Geographics*, 10(1), 15.
Fu, P., and Sun, J. (2010). *Web GIS: Principles and applications*, ESRI, Redlands, CA.
Gall, M., Boruff, B. J., and Cutter, S. L. (2007). "Assessing flood hazard zones in the absence of digital floodplain maps: Comparison of alternative approaches." *J. Nat. Hazards. Rev.*, 10.1061/(ASCE)1527-6988(2007)8:1(1), 1–12.
HEC-2 [Computer software]. U.S. Army Corps of Engineers—Hydrologic Engineering Center (HEC), Davis, CA.
HEC-GeoRAS [Computer software]. Esri, Redlands, CA.
HEC-RAS [Computer software]. U.S. Army Corps of Engineers—Hydrologic Engineering Center, Davis, CA.
Javadnejad, F. (2013). "Flood inundation mapping using HEC-RAS and GIS for Shelby County, Tennessee." M.S. thesis, Univ. of Memphis, Memphis, TN.
Javadnejad, F., Waldron, B. A., and Alinia, F. (2013). "GIS-based gold potential mapping in the Muteh deposit area, Iran, with respect to a new mineralization concept." *4th Int. Conf. on Computing for Geospatial Research and Application (COM. Geo)*, IEEE, Piscataway, NJ, 148–149.
Kashani, A., Olsen, M., Parrish, C., and Wilson, N. (2015a). "A review of LIDAR radiometric processing: From Ad Hoc intensity correction to rigorous radiometric calibration." *Sensors*, 15(11), 28099–28128.
Kashani, A. G., Crawford, P. S., Biswas, S. K., Graettinger, A. J., and Grau, D. (2015b). "Automated tornado damage assessment and wind speed estimation based on terrestrial laser scanning." *J. Comput. Civ. Eng.*, 10.1061/(ASCE)CP.1943-5487.0000389, 04014051.
Kiesel, J., Schmalz, B., and Fohrer, N. (2009). "SEPAL—A simple GIS-based tool to estimate sediment pathways in lowland catchments." *Adv. Geosci.*, 21(21), 25–32.
Kinzel, P. J., Legleiter, C. J., and Nelson, J. M. (2013). "Mapping river bathymetry with a small footprint green LiDAR: Applications and challenges." *J. Am. Water Resour. Assoc.*, 49(1), 183–204.
Malczewski, J. (2006). "Ordered weighted averaging with fuzzy quantifiers: GIS-based multicriteria evaluation for land-use suitability analysis." *Int. J. Appl. Earth Observ. Geoinform.*, 8(4), 270–277.
Manning, R. (1891). "On the flow of water in open channels and pipes." *Trans. Inst. Civ. Eng. Ireland*, 20, 161–207.
Molan, Y. E., and Behnia, P. (2013). "Prospectivity mapping of Pb–Zn SEDEX mineralization using remote-sensing data in the Behabad area, Central Iran." *Int. J. Remote Sens.*, 34(4), 1164–1179.
Moriasi, D. N., Arnold, J. G., Van Liew, M. W., Bingner, R. L., Harmel, R. D., and Veith, T. L. (2007). "Model evaluation guidelines for systematic quantification of accuracy in watershed simulations." *Trans.Am. Soc. Agric. Biol. Eng.*, 50(3), 885–900.
NOAA (National Oceanic and Atmospheric Administration). (2010). "Total of 14 Tornadoes from the May 1-2 Outbreak." ⟨http://www.srh.weather.gov/meg/?n=may122010severeweather⟩ (May 8, 2010).
NOAA (National Oceanic and Atmospheric Administration). (2011). "NOAA partnered guidelines for the development of AHPS flood inundation mapping." ⟨http://water.weather.gov/ahps/NOAA_AHPS_Guidelines_Final_2011_v3.pdf⟩ (May 30, 2016).
NOAA (National Oceanic and Atmospheric Administration). (2012a). "Climate and records for National Weather Service Memphis, TN records 1981-2010." ⟨http://www.srh.noaa.gov/meg/?n=climatenormals⟩ (Mar. 10, 2012).
NOAA (National Oceanic and Atmospheric Administration). (2012b). "Lidar 101: An introduction to lidar technology, data, and applications." NOAA Coastal Services Center, Charleston, SC.
NRC (National Research Council). (2007). "Elevation data for floodplain mapping." Washington, DC.
Ozdenerol, E., Huang, Y., Javadnejad, F., and Antipova, A. (2015). "The impact of traffic noise on housing values." *J. Real Estate Pract. Educ.*, 18(1), 35–53.
Peck, R., and Devore, J. L. (2011). *Statistics: The exploration and analysis of data*, Cengage Learning, Independence, KY, 464–465.
Pender, G., and Néelz, S. (2007). "Use of computer models of flood inundation to facilitate communication in flood risk management." *Environ. Hazards*, 7(2), 106–114.
Poff, N. L., et al. (1997). "The natural flow regime—A paradigm for river conservation and restoration." *BioScience*, 47(11), 769–784.
Singh, J., Knapp, H. V., Arnold, J. G., and Demissie, M. (2005). "Hydrologic modeling of the Iroquois River watershed using HSPF and SWAT." *J. Am. Water Resour. Assoc.*, 41(2), 343–360.
TEMA (Tennessee Emergency Management Agency). (2010). "May storms and flooding of 2010." ⟨http://www.tnema.org/events/index.html⟩ (May 30, 2016).
USACE (U.S. Army Corps of Engineers). (1995). "Wolf River reconnaissance report." Memphis, TN.
USGS. (2006). "Flood hazards—A national threat." ⟨http://pubs.usgs.gov/fs/2006/3026/2006-3026.pdf⟩ (May 29, 2016).
USGS. (2013). "U.S. Geological Survey flood inundation initiative: Prospectus." ⟨http://water.usgs.gov/osw/flood_inundation/files/USGS_Flood_Inundation_Prospectus_Final.pdf⟩ (May 29, 2016).
Van Arsdale, R., Waldron, B., Ramsey, N., Parrish, S., and Yates, R. (2003). "Impact of river channelization on seismic risk: Shelby County, Tennessee." *J. Nat. Hazards Rev.*, 10.1061/(ASCE)1527-6988(2003)4:1(2), 2–11.
Van Der Knijff, J. M., Younis, J., and De Roo, A. P. J. (2010). "LISFLOOD: A GIS-based distributed model for river basin scale water balance and flood simulation." *Int. J. Geog. Inform. Sci.*, 24(2), 189–212.
Verdin, J., et al. (2016). "A software tool for rapid flood inundation mapping." ⟨http://pubs.usgs.gov/of/2016/1038/ofr20161038.pdf⟩ (Jun. 4, 2016).
Willmott, C. J., and Matsuura, K. (1995). "Smart interpolation of annually averaged air temperature in the United States." *J. Appl. Meteor.*, 34(12), 2577–2586.
Yang, Z., Wang, T., Khangaonkar, T., and Breithaupt, S. (2012). "Integrated modeling of flood flows and tidal hydrodynamics over a coastal floodplain." *Environ. Fluid Mech.*, 12(1) 63–80.